

# A proposal for multi-tens of GW fully coherent femtosecond soft X-ray lasers

E. Oliva<sup>1</sup>, M. Fajardo<sup>2</sup>, L. Li<sup>1</sup>, M. Pittman<sup>3</sup>, T. T. T. Le<sup>1</sup>, J. Gautier<sup>1</sup>, G. Lambert<sup>1</sup>, P. Velarde<sup>4</sup>, D. Ros<sup>3</sup>, S. Sebban<sup>1</sup> and Ph. Zeitoun<sup>1\*</sup>

**X-ray free-electron lasers<sup>1,2</sup> delivering up to  $1 \times 10^{13}$  coherent photons in femtosecond pulses are bringing about a revolution in X-ray science<sup>3-5</sup>. However, some plasma-based soft X-ray lasers<sup>6</sup> are attractive because they spontaneously emit an even higher number of photons ( $1 \times 10^{15}$ ), but these are emitted in incoherent and long (hundreds of picoseconds) pulses<sup>7</sup> as a consequence of the amplification of stochastic incoherent self-emission. Previous experimental attempts to seed such amplifiers with coherent femtosecond soft X-rays resulted in as yet unexplained weak amplification of the seed and strong amplification of incoherent spontaneous emission<sup>8</sup>. Using a time-dependent Maxwell-Bloch model describing the amplification of both coherent and incoherent soft X-rays in plasma, we explain the observed inefficiency and propose a new amplification scheme based on the seeding of stretched high harmonics using a transposition of chirped pulse amplification to soft X-rays. This scheme is able to deliver  $5 \times 10^{14}$  fully coherent soft X-ray photons in 200 fs pulses and with a peak power of 20 GW.**

Over the past 10 years, the emergence of hard ( $\lambda \approx 0.1$  nm) and soft ( $\lambda \approx 4-30$  nm) X-ray free-electron lasers (FEL) with intensities rapidly increasing to  $1 \times 10^{18}$  W cm<sup>-2</sup> has led to scientific breakthroughs in a diverse number of fields<sup>3-5</sup>. This race has led to renewed interest in a specific class of soft X-ray lasers (XRLs) that use a plasma amplifier created by the interaction of a nanosecond, high-energy laser with a solid target. These XRLs routinely produce an extreme number of photons per pulse<sup>7</sup>, up to  $1 \times 10^{15}$  (that is, 10 mJ), which compares favourably with soft X-ray FELs, which emit a maximum of  $1 \times 10^{13}$  photons per pulse<sup>1,2</sup>. However, because these plasma-based XRLs are running in amplification of spontaneous emission (ASE) mode, they demonstrate weak coherence and long pulse durations (100 ps). Seeding these plasmas, which naturally emit up to 10 mJ, holds the greatest promise of producing fully coherent, femtosecond, multi-millijoule soft X-ray pulses. Such an experiment was carried out in 1995<sup>8</sup>, but this showed an as yet unexplained weak amplification of the seed (output, 100 nJ) and strong amplification of the ASE (reaching several millijoules). Plasmas created by femtosecond<sup>9</sup> to picosecond<sup>10</sup> infrared lasers have been seeded, but continue to be limited by the generation of long (picosecond) and low-energy (1  $\mu$ J) pulses. Numerical studies have shown that these schemes could amplify the seed to generate pulses of up to 70 fs (ref. 11), but with energy restricted to <40  $\mu$ J (ref. 12). It is only an in-depth study of Ditmire's seminal experiment<sup>8</sup> that holds the key to unlocking the path towards millijoule, femtosecond soft X-ray lasers.

The modelling parameters of our Maxwell-Bloch model<sup>13</sup> were adjusted on the basis of experiments<sup>8</sup> with a 200 fs, 0.5 nJ,

21.2 nm seed, and plasma with an electron density of  $4 \times 10^{20}$  cm<sup>-3</sup> and temperature of 550 eV. In the absence of seed, gain peaks at 25 cm<sup>-1</sup> were in good agreement with data from previous work<sup>14</sup>. Figure 1a shows the temporal evolution of the seed and ASE intensities at different locations ( $z$ ) along the plasma amplifier. The modelling reproduces the experimental data well: the amplified seed (Fig. 1a, red) is about twice as intense as the ASE (Fig. 1a, blue), and the ASE energy (5 mJ) dominates greatly over that of the amplified seed (11  $\mu$ J). This result highlights a key issue: plasmas pumped by long pulses lasting hundreds of picoseconds have intrinsic behaviours that contrast greatly with those of plasmas pumped by picosecond lasers<sup>9,10,12</sup>, with the latter exhibiting negligible ASE and very strong seed amplification ( $\sim 600$ ). This peculiar behaviour of millijoule-class XRLs can be understood only by examining the temporal response of the lasing ions to seed saturation (Fig. 1b). The gain drops to near zero when a strong seed is present, confirming deep saturation, but, in contrast to other XRLs where gain remains near zero, in millijoule-class plasmas, gain recovers fully after only 2 ps and then remains at its maximum value for  $\sim 2$  ns. This means that the seed pulse extracts the energy stored in population inversion during a period of less than 0.1% of the gain lifetime. In other words, more than 99.9% of the stored energy is not transferred to the coherent seed beam and is instead transferred to ASE. Accordingly, direct seeding with a femtosecond soft X-ray pulse into millijoule-class plasma, which is characterized by gain combining a long lifetime and fast recovery, is intrinsically inefficient.

We therefore studied two different schemes for coherently extracting the stored energy. The first, and straightforward, solution consists of seeding a train of femtosecond pulses separated by 2 ps throughout the entire gain duration. The parameters used to obtain Fig. 1a were used for modelling (Fig. 1c), except that a larger gain cross-sectional area<sup>7</sup> of  $4 \times 10^{-4}$  cm<sup>-2</sup> was applied. Using 100 seed pulses of 10 nJ each, the total energy at the plasma exit was divided into 7 mJ of amplified coherent seed and nearly 1 mJ of ASE. Figure 1d shows that the gain is fully saturated after amplification of each seed pulse, but recovers sufficiently to amplify the next pulse. Although the process shows a dramatic improvement in energy extraction with a coherent pulse, it is unrealistic to post-synchronize 100 soft X-ray pulses to achieve a single 7 mJ, 150 fs pulse. We therefore explored a second scheme, comprising extrapolation from this temporally discrete seed to a temporally continuous seed. This process is based on the use of a spatially and temporally coherent beam, but with pulse durations of hundreds of picoseconds, so that the energy can be extracted continuously, as quickly as it is restored. The seed duration in this case is now 200 ps, with 0.1  $\mu$ J energy, so that the seeding intensity is maintained far above the self-emission level. The temporal evolution

<sup>1</sup>LOA, UMR 7639, ENSTA-ParisTech, CNRS, Ecole Polytechnique-ParisTech, Chemin de la Hunière, F-91761 Palaiseau, France, <sup>2</sup>GoLP, Instituto de Plasmas e Fusão Nuclear, Laboratório Associado, Instituto Superior Técnico, Lisbon, Portugal, <sup>3</sup>CLUPS, EA4127, Bat 106, Université Paris-Sud, 91405 Orsay, France, <sup>4</sup>Instituto de Fusión Nuclear, Universidad Politécnica de Madrid, Madrid, Spain. \*e-mail: philippe.zeitoun@ensta-paristech.fr

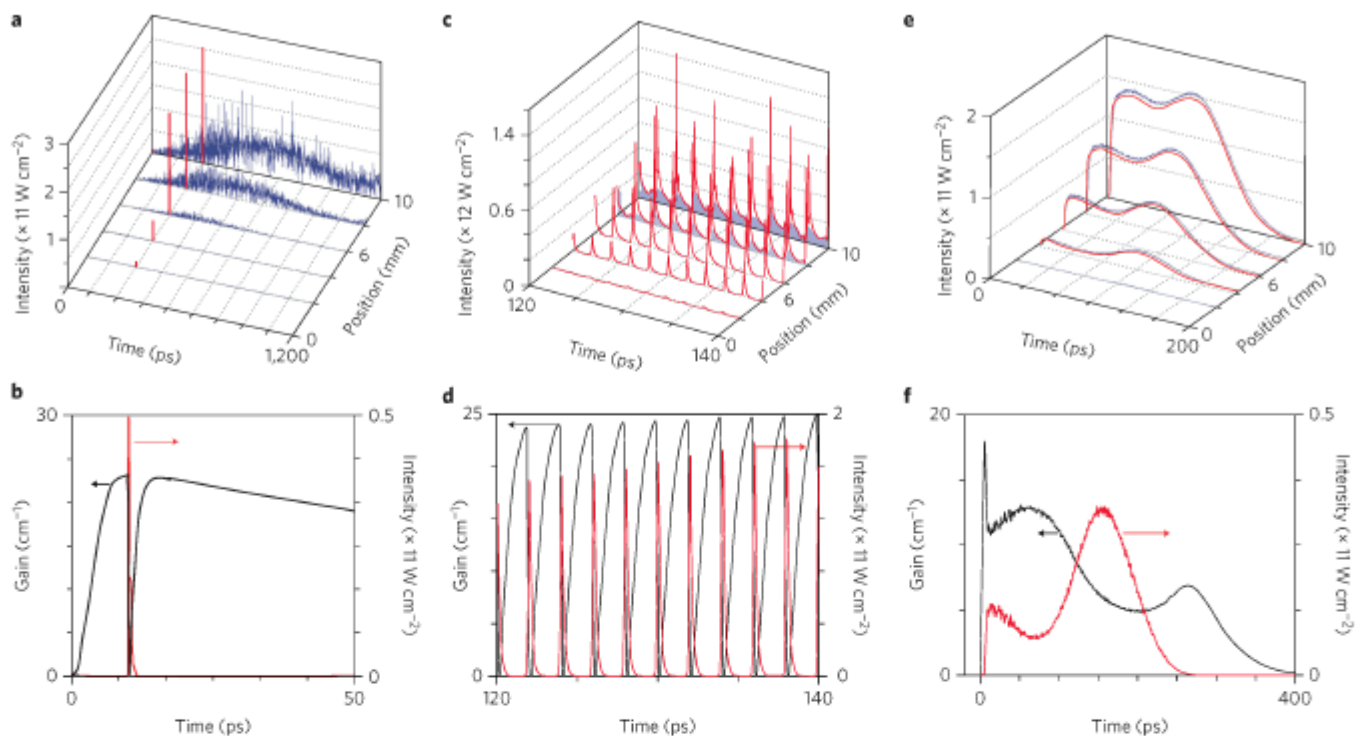


**Figure 1 | Temporal evolution of soft X-ray laser intensity and gain for different planes along the amplifier for single, multiple and stretched seeding.**

The coherent seed is in red and ASE in blue. **a,c,e.** Intensity curves, showing that the ASE spikes are very strong for a single seed (**a**), and barely visible for multi-pulse (**c**) (zoomed in time) and stretched (**e**) seeds, demonstrating that the output is dominated by a coherent signal. **b,d,f.** Gain (black) and intensity (red) at  $z = 4$  mm for cases **a, c** and **e**, demonstrating the efficiency of stretched seed amplification.

of intensity versus position along the amplifier is presented in Fig. 1e, and shows strong coherent seed amplification (10 mJ) and very weak ASE spikes (90  $\mu$ J). Long seed amplification yields a 1,000-fold enhancement of the coherent energy compared to femtosecond seeding and 30% more than when using a pulse train. Furthermore, the seed/ASE energy ratio after amplification is  $2 \times 10^{-3}$  for femtosecond seeds, 7 for a pulse train and 110 for stretched seed, demonstrating the optimized efficiency of this scheme.

Currently, our seed is composed of the high harmonics (HH) of femtosecond infrared lasers<sup>9,10</sup>. However, thus far, such HH has demonstrated only subpicosecond durations. We therefore proposed to generate a long HH pulse by transposing the chirped pulse amplification<sup>15</sup> technique to soft X-rays. Accordingly, the HH was stretched 1,000 times using a pair of commercially available gratings, then amplified and, thanks to the full temporal coherence of the high-harmonic seed, recompressed with another commercially available grating pair (Fig. 2a). Full details about the stretcher and compressor are provided in Supplementary Section ‘Stretcher and compressor design’. Recompression of the amplified stretched seed raises several issues. The seed spectral components must be phase-locked to retrieve to the Fourier limit, and HH has demonstrated such phase-locking<sup>16</sup>. In addition, the spectral phase after amplification must be regular. HH exhibits little phase distortion, and is responsible for only a few hundreds of attoseconds of broadening<sup>16</sup>, which is negligible compared to the 150 fs Fourier limit of millijoule-class XRLs. However, amplification of a pulse with a large spectrum generates phase distortion as a consequence of group velocity dispersion in the plasma. Indeed, in ref. 7, the plasma spectral phase deformation has been estimated to be 2 rad (Fig. 3a). Also, stretching the pulse by separating the spectral components in time introduces extra complexity into the amplification modelling, because the gain is not constant over time. The time-dependent gain at the centre-line calculated using our Maxwell–Bloch code

was therefore convolved with the XRL line shape (Fig. 3c). By including all these effects, we calculated the temporal pulse shape after compression (Fig. 2c) and observed a main pulse of 215 fs containing 97% of the energy. The pulse after recompression was advanced compared to the seed due to a slight asymmetry in the spectral gain (Fig. 2). It is worth noting that, due to the combination of fast gain regeneration and spectral stretching, the spectral components are amplified quasi-independently. Plasma XRLs, which are normally dominated by homogeneous broadening<sup>11</sup>, behave here like quasi-inhomogeneous lasers. Our preliminary calculations show that this characteristic opens the way to achieving 100 fs pulses by means of gain temporal shaping.

Finally, because the bandwidth of a single HH is estimated to be  $\sim 100$  times larger than the line width of the XRL from ref. 7, 1% of the energy is seeded into the XRL line at the plasma entrance. Considering a minimum seeding level of 0.1  $\mu$ J in-band, the HH energy has to be  $\sim 10$   $\mu$ J, which is orders of magnitude above the most energetic HH emitted around 20 nm. However, plasmas pumped by joule-class lasers may easily amplify 10 nJ HH up to the required level<sup>12</sup>. Figure 3a presents a full spectro-temporal energy calculation including group velocity dispersion, starting from a low-energy HH seed, passing through a plasma preamplifier, the stretcher and the main amplifier to produce a 10 mJ pulse.

We then considered a single-pass compressor and stretcher working with conical off-axis gratings, which experimentally demonstrated a diffraction efficiency as high as 70% around 20 nm (ref. 17). The total stretcher efficiency was estimated to be  $\sim 30\%$  (two 1,000  $\text{l mm}^{-1}$  gratings under 55.34° incidence and 7° altitude angles coupled by a grazing incidence telescope), and that of the compressor was 50% (same gratings and no telescope). Details are provided in the Supplementary Information. The output pulse can thus attain an unprecedented energy of 5 mJ ( $5 \times 10^{14}$  coherent photons) in 215 fs; that is, 100 times higher

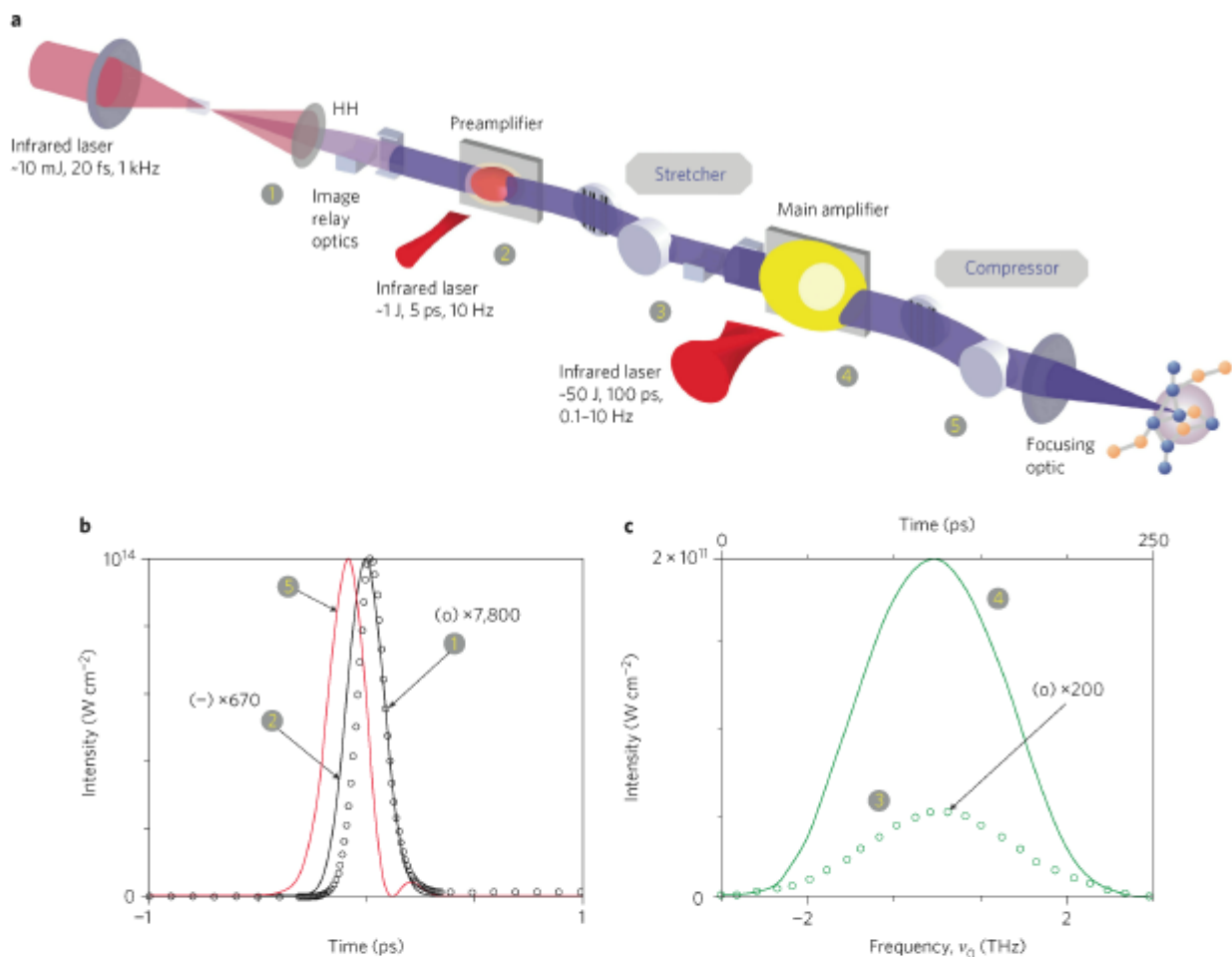


**Figure 2 | Artistic view of the stretched seed amplification chain with spectro-temporal evolution of the pulse along the chain. a**, Schematic of the amplification chain. **b**, Soft X-ray laser (SXRL) intensity versus time at the entrance of the preamplifier (symbols,  $\times 7,800$ ), at the exit of the preamplifier (black line,  $\times 670$ ) and after final amplification and compression (red line). The temporal shift is due to a slight asymmetry in spectral gain. **c**, Spectral intensity at the entrance (symbols,  $\times 200$ ) and exit (line) of the main amplifier. The numbers in **b** and **c** correspond to normalization factors.

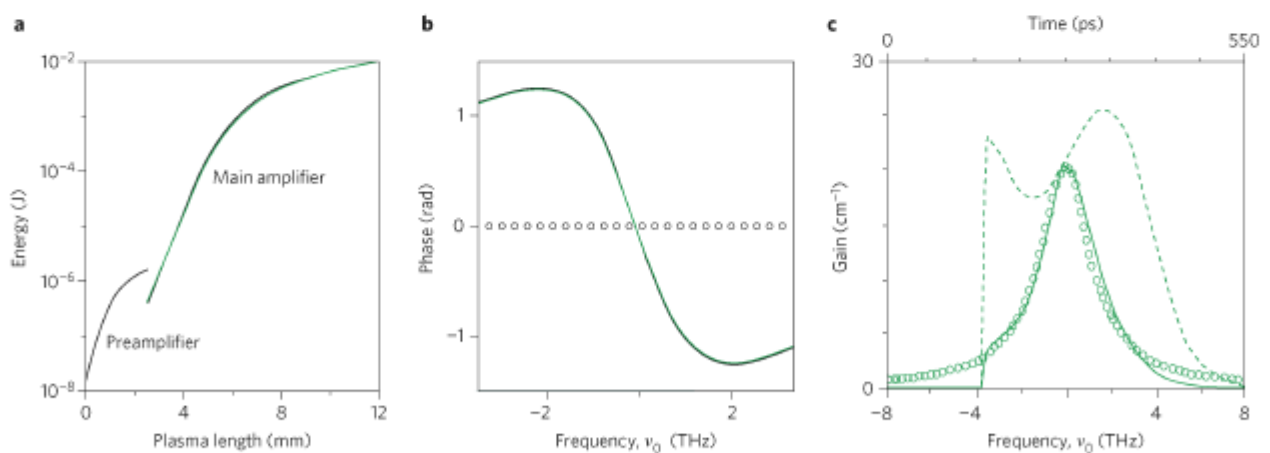


**Figure 3 | Modification of energy and spectral characteristics induced by the main amplifier. a**, Output energy versus plasma length for the pre- and main amplifiers. **b**, Spectral phase at the entrance (symbols) and exit (line) of the main amplifier. **c**, Gain (dashed green line) calculated by the time-dependent Maxwell-Bloch model, the spectral line shape (green line) and their convolution (green circles) when considering the use of an X-ray CPA stretcher.

than the best current soft X-ray FELs<sup>2</sup>. With a power of over 20 GW, these new soft X-ray lasers are 10,000 times more powerful than previous plasma-based XRLs. It is worth noting that using a

preamplifier and soft X-ray chirped pulse amplification (CPA) allows a dramatic reduction in the total pumping energy, from kilojoules previously<sup>7,8</sup> to  $\sim 100$  J. Furthermore, our detailed

calculations suggest the possibility of downscaling the long-HH seed scheme by using plasmas with gain durations at least longer than  $\sim 10$  ps (see Supplementary Information). The electron density has to be kept high to ensure a picosecond gain recovery time. Plasma tailoring by shaping the pump laser focal line in space would generate the appropriate conditions<sup>13</sup>. In such a case, no pre-amplifier is needed and both stretcher and compressor will be downsized to sub-metre scales. A downscaled version could be implemented at small-scale (hundreds of terawatts, 10 Hz) laser facilities to deliver soft X-ray pulses up to 0.5 mJ in 200 fs, equivalent to today's best soft X-ray FEL but fully coherent in space and time.

## Methods

Our time-dependent Maxwell–Bloch code solves the temporal variation of the amplification of both seed and spontaneous emission along the plasma column by dynamically coupling the population of the lasing levels with electromagnetic wave propagation and amplification<sup>18–20</sup>. Emission and amplification of spontaneous emission were incorporated self-consistently<sup>15,21</sup>. The evolution of the lasing ion population and seed beam electric field were treated in a fully time-dependent way, giving both the pulse duration and detailed temporal structure directly. The compressor and stretcher data were computed by solving conical diffraction formulae. Further details and explanations are given in the Supplementary Information.

## References

1. Emma, P. *et al.* First lasing and operation of an ångström-wavelength free-electron laser. *Nature Photon.* **4**, 641–647 (2010).
2. Ackerman, W. *et al.* Operation of a free-electron laser from the extreme ultraviolet to the water window. *Nature Photon.* **1**, 336–342 (2007).
3. Chapman, H. N. *et al.* Femtosecond diffractive imaging with a soft-X-ray free-electron laser. *Nature Phys.* **2**, 839–843 (2006).
4. Nagler, B. *et al.* Turning solid aluminium transparent by intense soft X-ray photoionization. *Nature Phys.* **9**, 693–696 (2009).
5. Young, L. *et al.* Femtosecond electronic response of atoms to ultra-intense X-rays. *Nature* **466**, 56–61 (2010).
6. Tallents, G. J. The physics of soft X-ray lasers pumped by electron collisions in laser plasmas. *J. Phys. D* **35**, R259–R276 (2003).
7. Rus, B. *et al.* Multimillijoule, highly coherent X-ray laser at 21 nm operating in deep saturation through double-pass amplification. *Phys. Rev. A* **66**, 063806 (2002).
8. Ditmire, T. *et al.* Amplification of XUV harmonic radiation in a gallium amplifier. *Phys. Rev. A* **51**, R4337–R4340 (1995).

9. Zeitoun, P. *et al.* A high-intensity highly coherent soft X-ray femtosecond laser seeded by a high harmonic beam. *Nature* **431**, 426–429 (2004).
10. Wang, Y. *et al.* Phase-coherent, injection-seeded, table-top soft-X-ray lasers at 18.9 nm and 13.9 nm. *Nature Photon.* **2**, 94–98 (2008).
11. Whittaker, D. *et al.* Producing ultrashort, ultraintense plasma-based soft-X-ray laser pulses by high-harmonic seeding. *Phys. Rev. A* **81**, 043836 (2010).
12. Oliva, E. *et al.* Optimization of soft X-ray amplifier by tailoring plasma hydrodynamics. *Opt. Lett.* **34**, 2640–2642 (2009).
13. Oliva, E. *et al.* Comparison of natural and forced amplification regimes in plasma-based soft-X-ray lasers seeded by high-order harmonics. *Phys. Rev. A* **84**, 013811 (2011).
14. Holden, P. *et al.* A computational investigation of the neon-like germanium collisionally pumped laser. *J. Phys. B* **27**, 341–367 (1994).
15. Strickland, D. & Mourou, G. Compression of amplified chirped optical pulses. *Opt. Commun.* **56**, 219–221 (1985).
16. Paul, P. M. *et al.* Observation of a train of attosecond pulses from high harmonic generation. *Science* **292**, 1689–1692 (2001).
17. Pascolini, M. *et al.* Gratings in a conical diffraction mounting for an extreme-ultraviolet time-delay-compensated monochromator. *Appl. Opt.* **45**, 3253–3262 (2006).
18. Hopf, F. A. & Scully, M. O. Theory of an inhomogeneously broadened laser amplifier. *Phys. Rev.* **179**, 399–416 (1969).
19. Armandillo, E. & Spalding, I. J. Pulse propagation of CO<sub>2</sub> laser amplifiers. *J. Phys. D* **8**, 2123–2135 (1975).
20. Sureau, A. & Holden, P. B. From amplification of spontaneous emission to saturation in X-ray laser: a Maxwell–Bloch treatment. *Phys. Rev. A* **2**, 3110–3125 (1995).
21. Larroche, O. *et al.* Maxwell–Bloch modeling of X-ray-laser-signal buildup in single- and double-pass configurations. *Phys. Rev. A* **62**, 043815 (2000).

## Acknowledgements

The authors thank G.J. Tallents, G. Mourou, J.P. Chambarret and V. Ceban for fruitful discussions. The work has been partially supported by SFINX-LASERLAB EC Seventh FP (grant agreement no. 228334) and the SHYLAX project from RTRA–Triangle de la Physique.

## Author contributions

The general concept was developed by P.Z., E.O. and M.F. Modelling was performed by E.O., P.V., P.Z. and T.T.T.L. Stretcher/compressor data were calculated by P.Z. and L.L., based on a model from M.P. and an idea from J.G. Detailed design and calculations were carried out with help from all authors.

## Additional information

Supplementary information is available in the online version of the paper. Reprints and permission information is available online at <http://www.nature.com/reprints>. Correspondence and requests for materials should be addressed to P.Z.

## Competing financial interests

The authors declare no competing financial interests.